# 6D.4 CHARACTERIZATION OF THE DYNAMICAL ROLE OF CONVECTION IN TWO SIMULATED EPISODES OF RAPID INTENSIFICATION

Daniel S. Harnos* and Stephen W. Nesbitt
Department of Atmospheric Sciences, University of Illinois at Urbana-Champaign, Urbana, Illinois

## 1. INTRODUCTION

Prediction of tropical cyclone (TC) rapid intensification (RI) represents one of the primary challenges facing the tropical meteorology community. It is accepted that the secondary circulation within the inner-core drives warm core development responsible for TC intensity change, as latent heat is released within the ascending circulation branch while the resulting subsidence branch yields further warming adiabatically. Recent works such as Vigh and Schubert (2009) and Pendergrass and Willoughby (2009) among others have used idealized vortices with prescribed heating to note the importance of heating position relative to the radius of maximum wind (RMW) location in the generation of the TC warm core due to the increased inertial stability occurring within the RMW.

Using 85 GHz brightness temperature Harnos and Nesbitt (2011) highlight two structural patterns associated with TCs undergoing RI dependent upon the environmental shear. The low-shear mode possesses widespread modest convection with ice processes surrounding the TC center while the high-shear mode is typified by more isolated, intense convection preferentially occurring right of the shear vector. Intense convection such as convective bursts (CBs) or hot towers have been frequently evaluated for their role in TC intensification, despite the lower-shear RI mode with less frequent CB contributions being more prevalent in the satellite record of Harnos and Nesbitt (2011). Due to the prevalence of the low shear RI mode, lesser magnitudes of convection merit investigation for their potential roles in intensification. Conversely to the Harnos and Nesbitt study, Kieper and Jiang (2012) highlight the potential importance of "warm rain and liquid clouds" in RI from 37 GHz observations.

In this study, an objective algorithm to quantify the 3-D RMW position is developed and applied to two simulated RI episodes for TCs under low (Hurricane Ike of 2008) and high (Hurricane Earl of 2010) wind shear. This objective RMW estimate is then used to define an analysis region for investigation of TC inner-core precipitation and associated heating characteristics that is superior to arbitrary TC inner-core definitions, due to the inherent physical importance of the heightened inertial stability existing within the RMW. A 3-D updraft metric is also developed to quantify individual updraft contributions toward intensification. Updraft maximum heights are used as a proxy for classification into varying regimes of convection (e.g. shallow cumulus, cumulus congestus, deep convection, and CBs).

*Corresponding author address: Daniel S. Harnos, Dept. of Atmos. Sci., Univ. of Illinois at Urbana-Champaign, Urbana, IL 61820; e-mail harnos1@illinois.edu

## 2. SIMULATION DESCRIPTIONS

### 2.1 *Simulation Setup*

Each simulation is performed with version 3.3 of the Weather Research and Forecasting (WRF) model Advanced Research WRF (ARW). Four domains are utilized at 27, 9, 3, and 1 km with the innermost domain following the TC via preset moves. All domains have 55 vertical levels with enhanced resolution within the boundary layer, near the freezing level, and outflow layer as in McFarquhar et al. (2012). Initial and boundary conditions come from the ECMWF's ERA-Interim reanalysis product. Parameterization choices include the Kain-Fritsch cumulus scheme (27 km domain only), WRF single-moment 6-class (WSM6) microphysics, Yonsei University (YSU) boundary layer scheme, and Rapid Radiative Transfer Model (RRTM) short- and long-wave radiation schemes. No vortex is prescribed for either simulation and the initial 24 h of each is discarded due to model spin up.

### 2.2 *Simulation Verification*

Each simulation is able to produce episodes of RI following the definition of a 30 kt/24 h by Kaplan and DeMaria (2003). Intensification is accelerated roughly 6 h in each model relative to observations, with Ike beginning RI at 18 UTC 2 September and Earl at 18 UTC 28 August. Discrepancies between simulated and observed track are generally within 1° at all times. Further, simulated ice water path values qualitatively mirror observed 89 GHz passive microwave structures at concurrent times near RI onset, suggesting the structure of the simulated TCs broadly mirrors observations. In the interest of space these results will be shown in the oral presentation.

## 3. RMW ALGORITHM

Studies evaluating TC inner-core precipitation typically utilize arbitrarily defined annuli for evaluation or otherwise quantify analyses relative to an axisymmetric RMW estimate at a singular height. Axisymmetric methods fail to account for asymmetries within the tangential wind field, which is observed to become increasingly symmetric with TC intensification (Croxford and Barnes, 2002). Despite this, observations show that the majority of TCs undergo RI while initially of tropical storm strength or weaker (Kaplan and DeMaria 2003; Harnos and Nesbitt 2011) which likely possess weak tangential wind fields. Further, RMW estimates at singular heights fail to account for tilt within a TC, which may be especially problematic for TCs such as Earl undergoing RI with environmental shear >5 m $s^{-1}$.

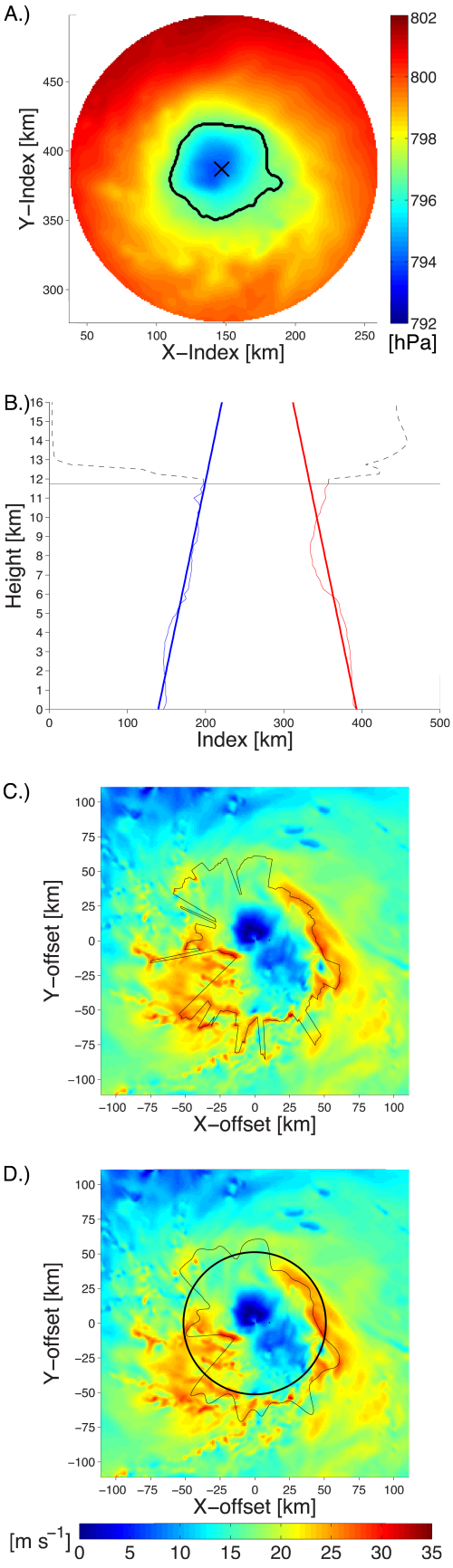


**Figure 1**: RMW algorithm example for Earl 18 UTC 28 August (see text for full description). (A) shows 2 km pressure with the largest pressure feature (black line) and its centroid (labeled x). (B) depicts the x-(thin blue line) and y-(thin red line) centers used for the least squares regression (thick lines) for describing the TC center. Dashed lines indicate values deemed irrepresentative. (C) shows the 2 km storm-realtive tangential wind field and initial RMW estimate (black line). (D) exhibits the final smoothed asymmetric RMW (thin line) and axisymmetric RMW (thick line).

An example of the objective 3-D RMW algorithm is depicted in Figure 1 at RI onset for the Earl simulation. First, a valid TC center is needed at all altitudes for decomposition of the wind into tangential and radial components. To determine the center the pressure field at 250 m altitude intervals is first smoothed 20 times with a 5x5 Gaussian filter. For the lowest level the SLP field is used and the 0.1$^{st}$ percentile of the pressure field then calculated. All regions below this percentile are flagged and the largest 4-sided contiguous region of such values is deemed to be representative of the TC, with the feature's centroid being the TC center. The next altitude layer is then processed over a circle with 1° radius relative to the anterior level's center with a similar procedure to encourage vertical consistency, except above the surface the 10$^{th}$ percentile of pressure is used instead (Fig. 1A). Once the column has centers initially evaluated through 16 km altitude, a least squares fit is taken of the initial centers over the region where the vertical variability of the x- and y-positions varies less than 10 km over 250 m altitude (Fig. 1B). This fit is deemed to represent the TC center with respect to height, and is used to derive tangential winds following removal of storm-motion from WRF output wind fields.

The RMW is assumed to lie within 5-111 km from the TC center. At all altitudes the tangential winds are evaluated along 1 degree radii over each 1° of azimuth, where along the radii a 1-3-1 filter is used to smooth any localized radial variability with the maximum smoothed wind value along the radial being deemed the initial RMW position (Fig. 1C). To limit strong azimuthal variability, further smoothing of the RMW occurs using a Gaussian filter twice along ±3° of azimuth at each height level. The resulting values are taken as the final RMW estimate (Fig. 1D). RMS errors of the axisymmetric RMW relative to the asymmetric RMW (Figure 2) are typically above 30 km throughout the vertical preceding RI for each simulation, indicating the limited utility of axisymmetric RMW estimates.

## 4. PRECIPITATION CHARACTER

In investigating the thermodynamic role of precipitation within the TC inner-core, diabatic heating is linked to warm core development and TC intensification through the secondary circulation. As such, inner-core diabatic heating signals can aid in diagnosing the manifestation of intensity change. Figure 3 depicts the net amount of diabatic heating occurring within the asymmetric RMW estimate with respect to height and

**Figure 2 (below):** RMS errors for axisymmetric RMW relative to asymmetric RMW estimates for Ike (A) and Earl (B).

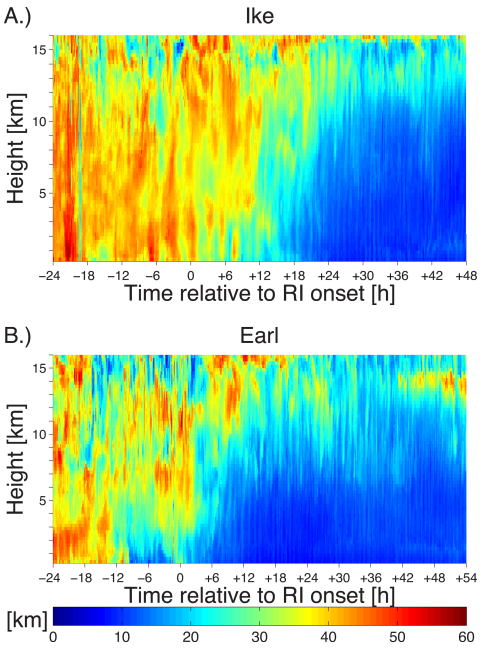


time. Both TCs exhibit absolute maxima in diabatic heating occurring within the RMW in the immediate vicinity of RI onset at magnitudes not witnessed again throughout the simulations. In Earl this maxima peaks between 5-11 km while for Ike the peak is between 5-8 km. With each of these peaks occurring above the freezing level, it points to the importance of ice processes in releasing latent heat (Zipser 2003) during RI. Throughout each time series, the diabatic heating is consistently stronger above the freezing level, due to the additional latent heat release associated with freezing hydrometeors.

To quantify potential importance of CBs in RI, the definition of Rogers (2010) is applied to quantify CB areal coverage within the asymmetric RMW of each TC in Figure 4. Ike (Fig. 4A) has unremarkable trends in CB areal coverage other than some minor maxima 24 h after RI has begun. Earl (Fig. 4B) is starkly different, with CB activity typically a factor of 4 more active than for Ike, with the CB activity enhanced through 12 h after RI has begun. CB activity in Earl peaks in the 6 h immediately following RI onset, coincident with the peak in aggregate diabatic heating within the RMW (Fig. 3B). The more prevalent CB signature in the high-shear RI case mirrors results from the satellite composites of Harnos and Nesbitt (2011).

## 5. VERTICAL MOTION CHARACTER

Prior studies such as Montgomery et al. (2006), Rogers (2010), and McFarquhar et al. (2012) among others have focused on CBs, however little work has been performed on convective magnitudes of lesser extent aside from Wang (2014). The CB definitions of

**Figure 3 (below)**: Aggregate diabatic heating within the asymmetric RMW for Ike (A) and Earl (B).

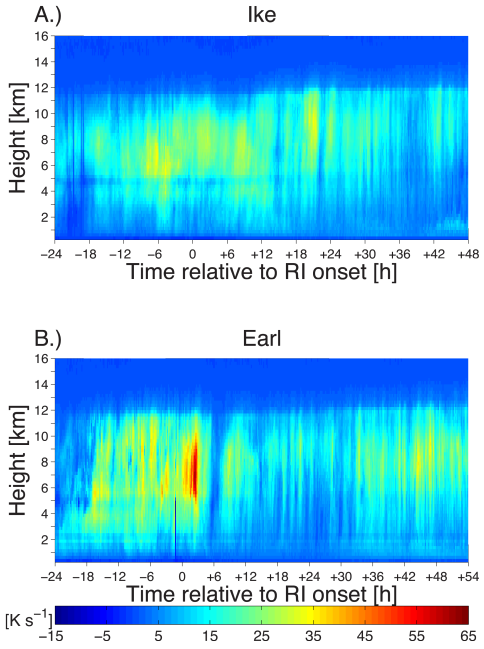


**Figure 4 (below)**: CB area following definition of Rogers (2010) within the asymmetric RMW of Ike (A) and Earl (B).

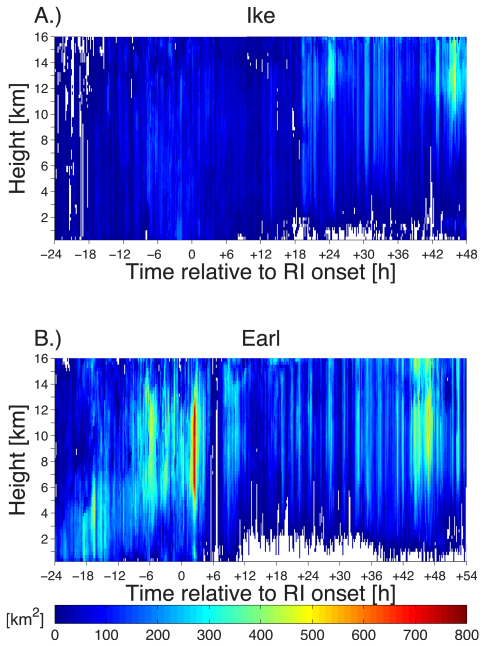


prior studies are limited however, due to their columnar nature ignoring vertical slope of updrafts coupled with the relatively small spatial extent of CBs *O*~10 km (Montgomery et al. 2006) that may result in CB contributions being underestimated. To better quantify precipitation contributions towards intensification, an

improved metric including a 3-D component of the vertical motion field is utilized through an analysis of updraft features. An updraft feature is defined as a 6-sided contiguous region where $W \geq 1$ m s$^{-1}$ extending over a minimum depth of 1 km. Updraft features are then classified according to their maximum altitude into convective regimes: updrafts reaching <5 km associated with shallow cumuli, >5 km but ≤8 km cumulus congestus, >8 km but ≤14 km deep convection, and >14 km CBs. We do not make an attempt to analyze regions with smaller vertical motions (e.g., those that would be associated with stratiform precipitation).

Figure 5 depicts the temporal evolution of relative contributions towards vertical mass flux within the RMW by each convective regime, noting strong contrasts between these two simulations preceding RI. For Ike (Fig. 5A) near RI onset vicinity mass flux contributions in order of importance are: deep convection, CBs, cumulus congestus, and shallow cumuli. Once CBs become well established within the RMW ~12 h after RI onset, they dominate mass flux through the remainder of the simulation. Vertical mass fluxes by shallow cumuli and cumulus congestus (both predominantly liquid phase) are generally below 30% near RI onset, again pointing to the role of ice phase processes in RI initiation. For the Earl simulation (Fig 5B), vertical mass flux is overwhelmingly dominated by CBs from ~12 h before RI begins through the end of the simulation, accounting for ≥90% of the vertical mass flux at nearly all times. For each simulation, the vertical vapor flux behaves similarly to the mass flux, with no evidence of shallow cumuli or cumulus congestus acting to precondition deep convection in either TC.

Diabatic heating contributions within the RMW can also be stratified according to convective regime as shown in Figure 6. The results mirror those of Figures 4 and 5, with the primary contributors towards diabatic heating being deep convection in Ike and CBs for Earl. The residual term (Fig. 6I,J) within each simulation accounts for updrafts <1 m s$^{-1}$ and evaporation or sublimation associated cooling within downdrafts. Ike (Fig. 6I) shows a clear stratiform profile within the residual term through 12 h following RI, with diabatic heating above the freezing level and cooling below it. Earl exhibits cooling below the freezing level but minimal warming above the freezing level that would indicate stratiform contributions (Houze et al. 1989). Apparent for Earl immediately prior to RI is cooling above the freezing level associated with sublimation, likely related to the wavenumber-1 asymmetric appearance of the precipitation field with drier air wrapping around the eastern side of the TC before RI.

## 6. SUMMARY

An objective method to quantify processes within TC inner-core using the asymmetric RMW position with respect to height is introduced for two WRF simulations of RI under low and high wind shear (Hurricanes Ike of 2008 and Earl of 2010 respectively). Using such an analysis framework allows for inherent physical

**Figure 5:** Relative proportion of vertical mass flux by updraft features classified via their maximum altitude within the asymmetric RMW of Ike (A) and Earl (B).

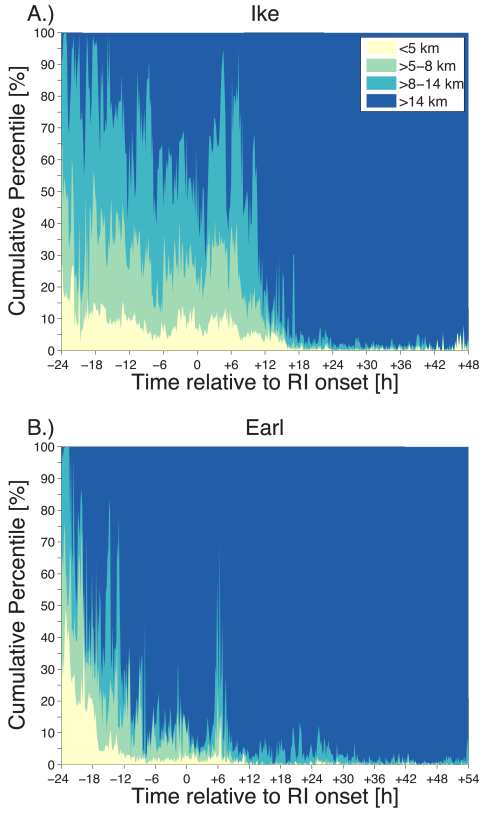


importance due to the highest inertial stability occurring within the RMW, thus allowing for more efficient warm core development, while also limiting potential contamination of inner-core analyses by features occurring outside of it as the RMW contracts over time. Consideration of RMW asymmetry is necessary for each simulation due to considerable RMS errors of above 30 km when using an axisymmetric approximation relative to the asymmetric value for nearly all times and altitudes preceding RI resulting from the weak vortex being readily modified by local convection. The RMW becomes reasonably axisymmetric ~12 hours after RI commencement for each TC, in line with observations by Croxford and Barnes (2002) of increasing axisymmetry with TC intensity.

Despite comparable intensifications by each storm, the thermodynamic roles of precipitation are starkly different for each TC. Within the asymmetric RMW absolute maxima in aggregate diabatic heating of >30 K s$^{-1}$ and >40 K s$^{-1}$ for Ike and Earl respectively are noted in the immediate vicinity of RI onset at altitudes above the freezing level, implicating the importance of ice processes in RI. This diabatic heating maxima is coincident with a peak in CB area within the RMW for the Earl simulation, while no such CB areal maxima occurs and overall burst activity in the vicinity of RI for Ike is smaller by a factor of 4.

**Figure 6:** Updraft feature contributions by individual convective regimes and residual term towards diabatic heating within the asymmetric RMW for Ike (A,C,E,G,I) and Earl (B,D,F,H,J).

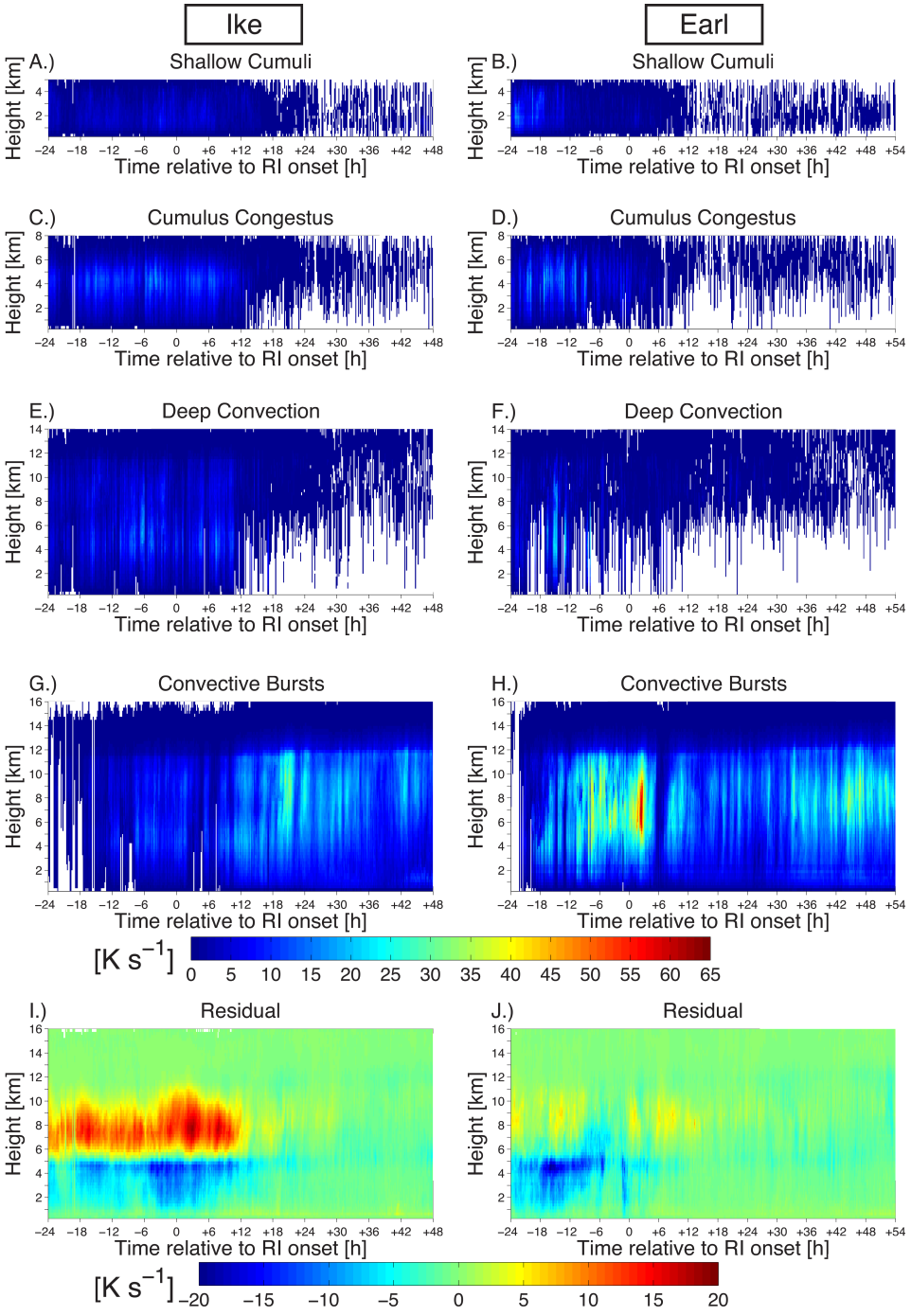


A metric utilizing 3-D updraft structure in order to quantify contributions towards convective regimes (i.e. shallow cumuli, cumulus congestus, deep convection, and CBs) relative to intensification is also developed. The Ike simulation sees vertical mass flux and diabatic heating contributions within the RMW primarily from deep convection followed by more intense CBs, cumulus congestus, and shallow cumuli while for Earl these contributions are overwhelmingly from CBs. The residual diabatic heating not accounted for by the convective regimes is reminiscent of stratiform precipitation for Ike through 12 h following RI onset while for Earl the upper level heating peak is substantially weaker, in agreement with the lack of stratiform rain processes. The importance of deep convection and CBs in the simulations points to the importance of ice phase

processes in RI and supports the satellite composite work of Harnos and Nesbitt (2011). These differences also point to clear differences in the intensification mechanisms in these two storms. The distinct stratiform precipitation signature, weak convection signatures, and lack of CBs in Ike also fail to align with the vortical hot tower intensification paradigm of Montgomery and Smith (2013), however further dynamical analyses are necessitated to confirm such results.

Additionally, muted signals are apparent for shallow cumuli and cumulus congestus in terms of contributions towards inner-core diabatic heating and vertical mass or vapor fluxes. Furthermore, environmental preconditioning for subsequent convection is not noted here as was described by Wang (2014). These results draw into question the importance of direct contributions of solely warm rain processes in RI, however the limitations of the modeling framework and the representativeness of these two storms in the general storm population needs further investigation. These results do suggest that exclusively warm rain processes and liquid clouds are neither a necessary nor sufficient condition for TC rapid intensification.

## 7. ACKNOWLEDGEMENTS

This project was funded by Ramesh Kakar under NASA HSRP Grant #NNX09AB82G and ESS Fellowship #NNX10AP50H. Computing resources were provided by the NASA Center for Climate Simulation.

## 8. REFERENCES

Croxford, M. and G. M. Barnes, 2002: Inner core strength of Atlantic tropical cyclones. *Mon. Wea. Rev.,* **130,** 127-139.

Harnos, D. S. and S. W. Nesbitt, 2011: Convective structure in rapidly intensifying tropical cyclones as depicted by passive microwave measurements. *Geophys. Res. Lett.,* **38,** L07805.

Houze, R. A., 1989: Observed structure of mesoscale convective systems and implications for large-scale heating. *Quart. J. Roy. Meteor. Soc.,* **115,** 425-461.

Kaplan, J. and M. DeMaria, 2003: Large-scale characteristics of rapidly intensifying tropical cyclones in the North Atlantic basin. *Wea. Forecasting,* **18,** 1093-1108.

Kieper, M. K. and H. Jiang, 2012: Predicting tropical cyclone rapid intensification using the 37 GHz ring pattern identified from passive microwave measurements. *Geophys. Res. Lett.,* **39,** L13804.

McFarquhar, G. M., B. F. Jewett, M. S. Gilmore, S. W. Nesbitt, and T.-L. Hsieh 2012: Vertical velocity and microphysical distributions related to rapid intensification in a simulation of Hurricane Dennis (2005). *J. Atmos. Sci.,* **69,** 3515-3534.

Montgomery, M. T., M. E. Nicholls, T. A. Cram, and A. B. Saunders, 2006: A vertical hot tower route to tropical cyclogenesis. *J. Atmos. Sci.,* **63,** 355-386.

Montgomery, M. T., and R. K. Smith, 2013: Paradigms for tropical cyclone intensification. *Aust. Meteor. Ocean. J.*, in press.

Pendergrass, A. G. and H. E. Willoughby, 2009: Diabatically induced secondary flows in tropical cyclones. Part I: Quasi-steady forcing. *Mon. Wea. Rev.,* **137,** 805-821.

Rogers, R., 2010: Convective-scale structure and evolution during a high-resolution simulation of tropical cyclone rapid intensification. *J. Atmos. Sci.,* **67,** 44-70.

Vigh, J. L. and W. H. Schubert, 2009: Rapid development of the tropical cyclone warm core. *J. Atmos. Sci.,* **66,** 3335-3350.

Wang, Z., 2014: Role of cumulus congestus in tropical cyclone formation in a high-resolution numermical model simulation. *J. Atmos. Sci.,* in press.

Zipser, E. J., 2003: Some views on “hot towers” after 50 years of tropical field programs and two years of TRMM data. *Meteor. Monogr,* **29,** 49-58.